Geophysical Research Letters

RESEARCH LETTER
10.1029/2020GL090499

Linear Relation Between Shifting ITCZ and Dust Hemispheric Asymmetry

Stuart Evans[1,2], Eliza Dawson[3], and Paul Ginoux[4]

[1]Department of Geography, University at Buffalo, Buffalo, NY, USA, [2]RENEW Institute, University at Buffalo, Buffalo, NY, USA, [3]Department of Geophysics, Stanford University, Stanford, CA, USA, [4]Geophysical Fluid Dynamics Laboratory, Princeton, NJ, USA

Key Points:
- Hemispherically asymmetric dust emission produces asymmetric radiative forcing that shifts tropical precipitation
- Increasing dust forcing in the Northern Hemisphere shifts the ITCZ linearly southward in the Atlantic, Pacific, and globally
- Millenial-scale dust variability from ocean sediment cores imply dust responsible for ~15% of shift in Atlantic ITCZ since the LGM

Supporting Information:
- Supporting Information S1

Correspondence to:
S. Evans,
stuartev@buffalo.edu

Citation:
Evans, S., Dawson, E., & Ginoux, P. (2020). Linear relation between shifting ITCZ and dust hemispheric asymmetry. *Geophysical Research Letters*, *47*, e2020GL090499. https://doi.org/10.1029/2020GL090499

Received 23 AUG 2020
Accepted 4 NOV 2020
Accepted article online 9 NOV 2020

Abstract Mineral dust is emitted primarily from arid regions, which may shrink or expand in one or both hemispheres, producing a complex and asymmetric pattern of radiative forcing that varies on interannual to millennial timescales. We assess the impact of hemispheric dust asymmetry on tropical precipitation. Using the Geophysical Fluid Dynamics Laboratory (GFDL) coupled climate model CM3 to simulate dust emission, we vary source strength in each hemisphere individually. Hemispherically asymmetric dust emission produces asymmetric dust load and radiative forcing. We find that the Intertropical Convergence Zone (ITCZ) shifts away from the hemisphere with enhanced dust load in response to the forcing asymmetry. We find significant linear relationships between the hemispheric imbalance and the latitude of tropical precipitation globally, in the Pacific, and especially in the Atlantic basin. This relationship offers a first-order estimation of dust effects on the hydrological cycle when investigating records of paleodust and for accurately predicting dust effects and feedbacks on future climate.

Plain Language Summary Dust aerosols in the climate system come from desert regions that are unevenly distributed across the globe. Currently, this unevenness produces much more dust in the Northern Hemisphere than in the Southern, but in previous climates, the degree of unevenness has varied. The presence of dust affects atmospheric energy balance by reflecting sunlight and absorbing infrared radiation. One consequence of an atmospheric energy imbalance is that the band of intense tropical rainfall near the equator shifts northward or southward. Using a global climate model, we increased and decreased the amount of dust in each hemisphere independently, creating a range of uneven dustiness and energy imbalance, and studied the tropical rainfall response. We found that tropical rainfall shifts away from the dustier hemisphere in a predictable way over both the Atlantic and Pacific oceans. The shift is especially strong over the Atlantic because it is downwind of the Sahara desert, the largest source of dust. Comparing our findings to records from the last ice age shows that dust accounts for roughly 15% of the shift of rainfall over the Atlantic since then. This dust-rainfall relationship may also help predict changes to the location of tropical rainfall in the future.

1. Introduction

Aerosols, including mineral dust, alter the climate both directly, by absorbing and scattering solar and terrestrial radiation, and indirectly, by modifying cloud physical and radiative properties, and precipitation processes. Scattering aerosols such as sulfate cool the climate while absorbing aerosols such as black carbon warm the climate. Dust both scatters and slightly absorbs solar radiation (Balkanski et al., 2007; Claquin et al., 1998), which reduces the radiative flux at the surface and heats the atmospheric column. In addition, dust absorbs terrestrial longwave radiation and re-emits it at a lower temperature, further warming the atmosphere (Ginoux, 2017). At the top of the atmosphere (TOA), the scattering effect of dust dominates, making dust a cooling agent over all but the brightest surfaces. Dust indirectly affects the climate by serving as cloud condensation nuclei and ice nuclei (Hoose et al., 2008), thereby changing the properties of clouds and influencing both radiative balance and precipitation. All of these changes to the energy balance of the atmosphere have the capacity to induce circulation changes, both local and global, that in turn can alter precipitation patterns.

The largest and most active dust sources are located in the Northern Hemisphere, mainly in a broad "dust belt" extending over several continents (Prospero et al., 2002). The Southern Hemisphere, with less land mass and fewer active sources, emits much less dust. Such contrast in dust emission generates a hemispheric asymmetry in atmospheric dust load and thus in radiative forcing as well (Miller et al., 2004). There is strong evidence that desert dust emission has experienced large variations in the past due to changing climate conditions, and the hemispheric asymmetry has been magnified or weakened on decadal (Prospero & Lamb, 2003) to millennial timescales (Fuhrer et al., 1999). Between glacial and interglacial periods dust deposition, a measure of the atmospheric concentration at the record site has changed by a factor of 3–4 globally and by up to a factor of 20 in polar regions (Kohfeld & Harrison, 2001). Comparison of the time series of dust concentration between ice cores from the Greenland Ice Core Project (GRIP) (Fuhrer et al., 1993) and the Project for Ice Coring in Antarctica (EPICA) Dome C (Fischer et al., 2007) reveals an order of magnitude difference between hemispheres, as well as asynchronous changes (e.g., during the Younger Dryas) since the Last Glacial Maximum (LGM). This asynchronous change generated additional asymmetry of dust load between hemispheres. During the mid-Holocene, when North Africa was very wet, dust production ceased completely from the Bodélé depression (Washington et al., 2006), presently the most active dust source on Earth (Ginoux et al., 2012). During this time, the Earth experienced a large shift in dust load and dust forcing from the Northern to Southern Hemispheres, weakening the hemispheric asymmetry. More recently, the hemispheric dust asymmetry shifted northward in the 1970s. Observed concentrations of African dust at Barbados in the Caribbean increased by a factor of 4 in the 1970s (Prospero & Lamb, 2003), while dust activities weakened by a factor of 3 at the same time in Australia (McTainsh et al., 2007), the Southern Hemisphere's most active dust source (Ginoux et al., 2012). Together, these changes represented a large shift in the relative dust load from the Southern to Northern Hemispheres.

Hemispheric dust asymmetries produce differential radiative forcing which in turn produces changes in surface temperature, precipitation and the general circulation. There is a strong literature demonstrating that cooling or heating one hemisphere relative to the other produces cross-equatorial energy transport that shifts the Intertropical Convergence Zone (ITCZ) toward the warmer hemisphere (e.g., Broccoli et al., 2006; Chiang & Bitz, 2005; Donohoe et al., 2013; Kang et al., 2008, 2009). The atmosphere responds to the imposed anomalies by transferring energy in the form of heat to the cooler hemisphere via the upper branch of the Hadley cell. The compensating low-level flow brings moisture in the opposite direction. As the Hadley cell shifts further into the warmer hemisphere, it transports more heat across the equator. In doing so, it shifts the location of the ITCZ and its associated rainfall toward the warmer hemisphere. This concept has been shown to explain ITCZ changes in both the paleo record (Chiang et al., 2003; Jacobel et al., 2016) and global warming scenarios (Frierson & Hwang, 2012). Kang et al. (2014), further demonstrated that the latitude of imposed warming and cooling affects the meridional structure of the tropical precipitation response. In their study, high-latitude forcings produced zonally symmetric precipitation responses, while tropical forcings produced precipitation responses in the vicinity of the forcing. Major dust sources, including North Africa and Australia, are located in subtropical and tropical regions; this implies that dust radiative forcing may have stronger impacts on the local ITCZ. Such a shift may alter wind and rainfall at the dust source, constituting a feedback on dust emission.

Considering the large variability of atmospheric dust load and its primarily cooling properties, we demonstrate how varying levels of dust influence the latitudinal position of the ITCZ and the associated precipitation band. Previous modeling studies have found ITCZ shifts due to other aerosol forcing agents such as sulfate (Hwang et al., 2013) and black carbon (Allen et al., 2012), but to the best of our knowledge, such a study has not been performed for an aerosol that both scatters and absorbs, such as dust. Marine sediment records suggest that during times of increasing Northern Hemisphere dust load the ITCZ moved southward in both the Atlantic (Adkins et al., 2006) and Pacific (Jacobel et al., 2016) basins. Conversely, when African dust emission is reduced, precipitation migrates northward in both models (Evans et al., 2019; Pauseta et al., 2016) and observations (McGee et al., 2013; Reimi & Marcantonio, 2016). In this study, we develop simulations to model the effect of hemispheric dust asymmetries by multiplying dust emission in one hemisphere or both by 0, 2, and 5 times preindustrial levels and examine the effects on tropical precipitation. In doing so, we create a suite of simulations with a wide range of dust asymmetries that allow for the characterization of the global response to changes in hemispheric dust forcing. While hemispheric dust emission in the past was never truly zero, a subset of these simulations serves as broadly analogous cases for dust asymmetries that existed in different climates and can be used to understand the effects of dust spatial variability during not only the present but periods such as the LGM, the African Humid Period, and future scenarios.

Further, by quantifying the relationship between relative dust load and ITCZ latitude, we make it possible to translate paleorecords of dust deposition into shifts of tropical precipitation.

2. Methods

This study uses the Geophysical Fluid Dynamics Laboratory (GFDL) coupled climate model CM3 (Donner et al., 2011), a fully coupled atmosphere-ocean-land-sea-ice model. Dust emission is calculated in the land model component of the model and is parameterized as a function of soil moisture, erodibility, bareness, and friction velocity as formulated by Evans et al. (2016, 2019). Once in the atmosphere, dust absorbs and scatters both shortwave and longwave radiation and is transported by advection, convection, and vertical diffusion. Optical properties (mass extinction efficiency, single scattering albedo, and asymmetry parameter) are calculated for spherical dust particles using simulated size distribution and the refractive index of a 2.7% hematite content derived by Balkanski et al. (2007). In CM3, dust may affect warm cloud properties in remote regions where sulfate concentration is low but will not act as ice condensation nuclei (see Donner et al., 2011, for details).

Certain model choices and limitations may have had limited effects on our results. For our simulations, we have assumed one set of optical properties, but dust mineralogy changes spatially (Claquin et al., 1999; Di Biagio et al., 2017), the particles may be not as coarse as observed (Kok et al., 2017), in addition to misrepresentation of dust transport and removal (Huneeus et al., 2011). Uncertainty in the mineralogy and size distribution of dust aerosols creates bias in the magnitude of the dust direct radiative effect. Previous studies of dust effects have dealt with this uncertainty by performing sensitivity studies of dust optical properties (Miller et al., 2004) or mineralogy (Li et al., 2020). Dust that is more scattering, either by mineralogy or by smaller size, creates greater precipitation reductions than dust that is more absorbing (Strong et al., 2015). Dust with sufficiently absorptive properties could change the sign of our results; however, the optical properties of the dust in our model are toward the absorbing end of uncertainties (Li et al., 2020; Strong et al., 2018) and more absorbing properties (Patterson et al., 1977; Volz, 1973) have been shown to be too absorptive (Sinyuk et al., 2003). This makes our results a low estimate. The lack of a dust indirect effect may limit the magnitude of our results. Sagoo and Storelvmo (2017) found that the ice nucleating indirect effect of dust suppressed tropical precipitation in CAM5.1. Such an effect would serve to amplify the relationship we find below, with the hemisphere with greater dust concentrations experiencing a greater reduction in tropical precipitation.

The model was run for 200 years with constant preindustrial forcings then branched into 10 different experiments with varying dust source strength. We vary dust source strength by using scaling factors of 0, 1, 2, or 5 times the control value, either in a single hemisphere or in both. The simulations are labeled according to the value of the multiplier in each hemisphere, for example, N0S0 indicates no source in both hemispheres while N5S5 means scaling of both hemispheres by 5. Our full set of experiments include N0S0, N1S0, N2S0, N5S0, N0S1, N0S2, N0S5, N2S2, and N5S5, as well as the control N1S1. Each of these experiments was run for 100 years, again with preindustrial forcings, and then averaged over the last 40 years. In order to examine the impact of different amounts of dust, we look at the difference between the experiments with altered source strength and the control.

3. Results

Figure 1 shows the change in dust optical depth for a selection of experiments relative to the N1S1 control. The N0S0 experiment (Figure 1a) essentially shows the optical depth of the control simulation, as the dust optical depth of N0S0 is, by definition, zero. When Southern Hemisphere dust emission is increased by a factor of five (Figure 1b), the dust optical depth increases slightly throughout the Southern Hemisphere, with a maximum increase of more than an optical depth over the source regions of Australia (Figure 1b) compared to the control run. Similarly, when the dust emission in the Northern Hemisphere is increased fivefold (Figure 1c), dust optical depth increases throughout the Northern Hemisphere, up to nearly two optical depths over north Africa. The dust load changes in the Northern Hemisphere are much greater than the dust load changes in the Southern Hemisphere as a result of there being both stronger and much more extensive dust sources in the Northern Hemisphere. The impact of this asymmetry can be seen in Figure 1c, where substantial parts of the Southern Hemisphere experience an increase in dust optical depth even when southern emission is set to zero because of the large increase in dust from the Northern Hemisphere.

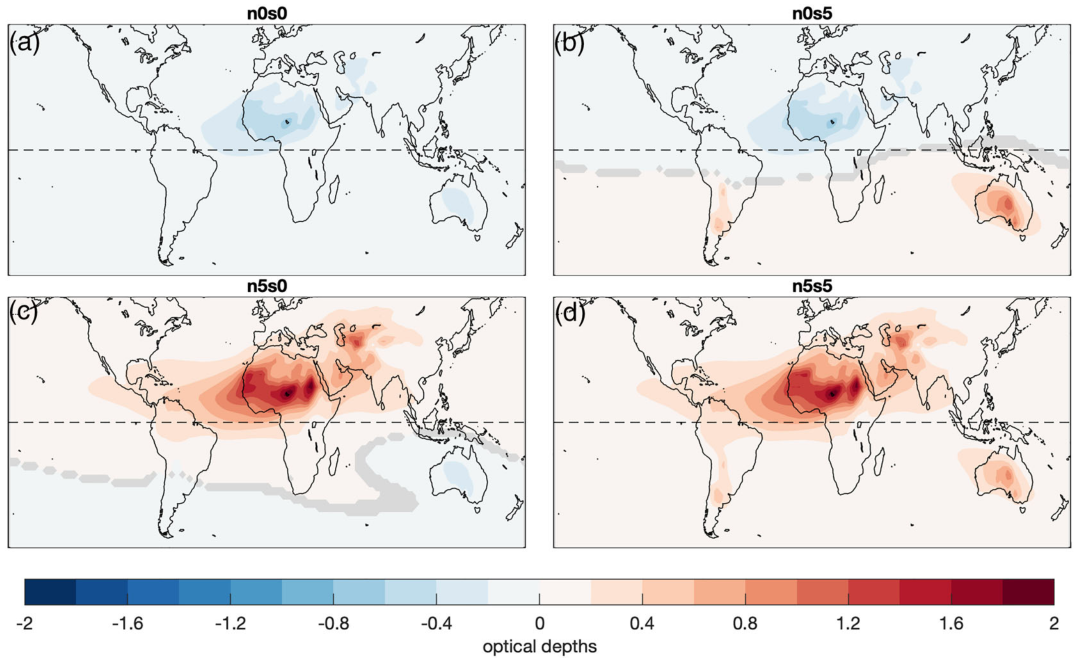

Figure 1. Change in mean dust optical depth for extreme dust emission simulations compared to the control experiment. Gray regions indicate lack of statistical significance (95% confidence), determined by a two-tailed *t*-test: (a) no dust emission, (b) no dust emission in the north and five times dust emission in the south, (c) five times dust emission in the north and no dust emission in the south, and (d) five times dust emission in both hemispheres.

Aerosol direct radiative forcing at the TOA responds to the dust optical depth (Figure 2). Asymmetric dust loading results in similarly asymmetric radiative forcing. While the longwave forcing of dust is positive everywhere due to its longwave absorption (Figure S1 in the supporting information), the strength of the shortwave forcing depends on the relative albedo of the dust and the surface beneath it (Figure S2). In most locations, the shortwave forcing dominates, and the radiative forcing becomes more negative as dust concentrations increase. Over sufficiently reflective surfaces however, the shortwave forcing becomes weak, and the total forcing becomes positive due to a dominant longwave effect. As a result, the high desert albedo of the Sahara produces a positive radiative forcing for increased dust (Figures 2c and 2d) and negative radiative forcing for decreased dust (Figures 2a and 2b). In contrast, over the ocean and darker land surfaces (including some deserts such as Australia) where the surface albedo is lower, there is always an increase of outgoing radiative flux by dust scattering. The magnitude of these radiative forcings can be large. When dust emission in the Northern Hemisphere is increased by a factor of 5, we see a negative radiative forcing over the Atlantic of up to 16 W/m^2 and a positive radiative forcing over northern Africa of up to 10 W/m^2 (Figure 2c). The pattern of forcing is consistent with the results of Miller et al. (2004), although their values are smaller as they did not amplify dust emission.

Tropical precipitation shifts southward as the radiative forcing from increased dust emission increases in the Northern Hemisphere and shifts northward as the radiative forcing increases in the Southern Hemisphere (Figure 3). We characterize the shift in tropical precipitation by calculating the precipitation centroid, θ, defined in Frierson and Hwang (2012) as the latitude of the median of the zonally averaged precipitation from 20°S to 20°N, such that

$$\int_{-20}^{\theta} \text{precip} = \int_{\theta}^{20} \text{precip}. \qquad (1)$$

We characterize the hemispheric imbalance in dust forcing by integrating the TOA aerosol radiative forcing (Figure 2) over each hemisphere and calculating the difference between the northern and southern hemispheres.

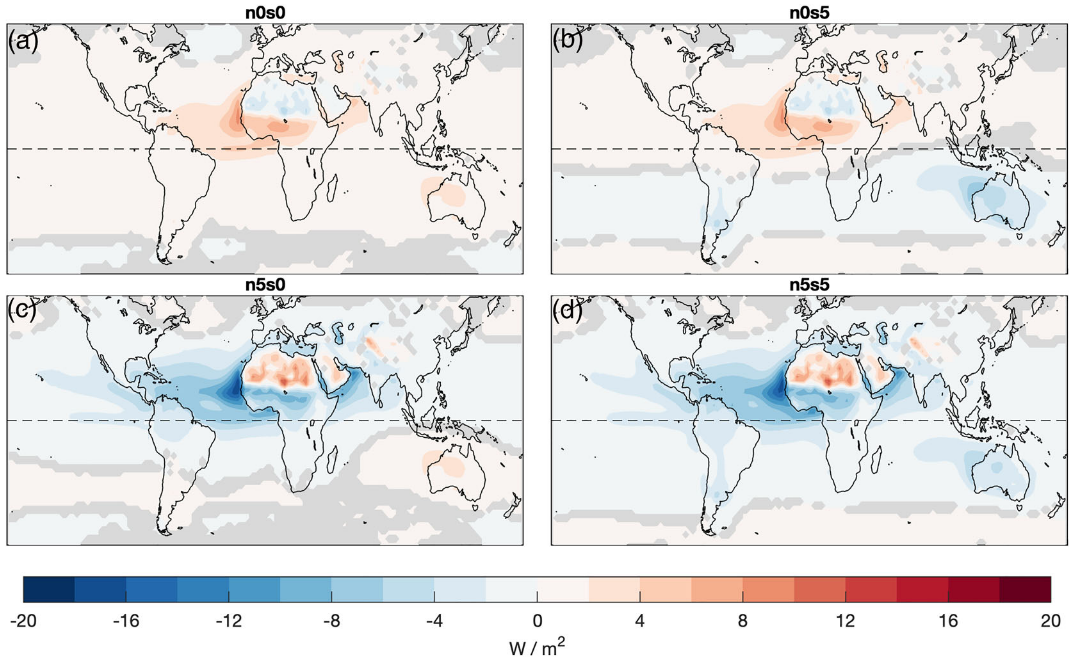

Figure 2. Same as Figure 1 but for all-sky aerosol direct radiative forcing at the top of the atmosphere. Aerosol radiative forcing is calculated as the difference in net flux between all-sky and clean-sky (i.e., aerosol-free) conditions.

$$\text{TOA Asymmetry} = \int_{0}^{90} (\text{TOA rad. forcing}) - \int_{-90}^{0} (\text{TOA rad. forcing}). \tag{2}$$

Figure 3 shows that our control (N1S1) has little asymmetry in dust radiative forcing. As dust load increases in the Northern Hemisphere, this metric becomes increasingly negative, and experiments appear to the left of the control simulation in Figure 3. We find that the precipitation centroid shifts away from the hemisphere with increased dust load, with the most southerly precipitation centroid occurring in the N5S0 simulation. The centroid shift is not zonally symmetric, with the strongest shift in precipitation occurring in the tropical Atlantic, where the precipitation centroid shifts by 2.0° across the suite of experiments, more than double the global range (0.8°). We confirm that the global shift is not simply due to the Atlantic sector by

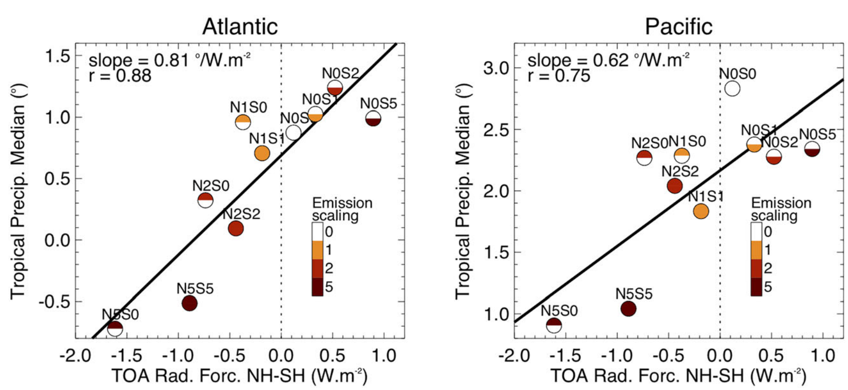

Figure 3. Shifts in tropical precipitation in response to hemispheric imbalance of TOA aerosol radiative forcing. Precipitation measured as the latitude of the median of tropical precipitation (20°S–20°N). Left panel shows tropical precipitation in the Atlantic sector (50°W–10°W), right panel tropical precipitation in the Pacific sector (150°E–100°W). The emission factors for each experiment are color coded for each hemisphere from zero (white filling) to 5 times (dark brown filling) the emission of the control run (N1S1).

Table 1
Linear Regression Slopes Between the Global, Atlantic (50°W–10°W), Indian (50°E–95°E), and Pacific (150°E–100°W) Tropical Precipitation Centroid and the Hemispheric (180°E–180°W Used for All Columns) Asymmetry in TOA Aerosol Radiative Forcing (Top Row) or Dust Emission Scaling Factor (Lower Rows)

	Global	Atlantic	Indian	Pacific
Hemispheric radiative forcing asymmetry (NH-SH)	**0.27°/Wm^{-2}**	**0.81°/Wm^{-2}**	0.11°/Wm^{-2}	**0.62°/Wm^{-2}**
Global dust emission scaling	**−0.13°/unit**	**−0.29°/unit**	−0.03°/unit	*−0.31°/unit*
Northern Hemisphere dust emission scaling	**−0.16°/unit**	**−0.35°/unit**	**−0.09°/unit**	**−0.37°/unit**
Southern Hemisphere dust emission scaling	−0.00°/unit	0.01°/unit	0.02°/unit	−0.07°/unit

Note. Negative values indicate southward shifts. Bold font indicates slopes that are significant at the 95% confidence level. Italics indicate 90% confidence.

finding the shift is statistically significant globally as well as in the Atlantic and Pacific basins individually (Table 1). The only ocean basin that does not experience a significant shift of the precipitation centroid is the Indian ($p = 0.14$).

We interpret these precipitation shifts as being due to a global shift in response to the asymmetry of hemispheric forcing with an additional regional shift in the Atlantic sector in response to changes in the nearby Saharan dust load. To confirm our interpretation of the global shift of the precipitation centroid as a response to the hemispheric forcing asymmetry, we also compare the location of the precipitation centroid to the cross-equatorial atmospheric heat flux as in Donohoe et al. (2013). We find a statistically significant shift of −4.4°/PW, indicating that the southward shift of the precipitation centroid can be explained by an ITCZ shift with the accompanying change in atmospheric heat flux. This value compares well with Donohoe et al. (2013) who reported precipitation shifts for anthropogenic and paleoclimatic forcing of −3.2 to −4.2°/PW. The Atlantic experiences a larger magnitude shift in the precipitation than the globe (Table 1). This is likely due to the nearby presence of the Sahara desert, the largest source of radiative forcing in our experiments. In the N5S0 experiment, the dust forcing produces strong surface cooling of over 1°C in the tropical Atlantic and up to 3°C close to the source regions (not shown). This cooling inhibits convection beneath the dust plume, primarily west Africa and the north tropical Atlantic. In doing so, it further shifts the balance of tropical precipitation to the south.

4. Discussion

Our results show that dust plays a significant role in determining the distribution of tropical precipitation. Hemispheric dust asymmetries alter the radiative balance of the atmosphere, generating an interhemispheric transfer of energy and a shift in precipitation along the ITCZ. We find significant linear relationships between increasingly negative dust forcing in the Northern Hemisphere and a southward shift of tropical precipitation globally, as well as in the Atlantic and Pacific basins individually. This relationship is stronger in the Atlantic than elsewhere because the largest source of dust is the Sahara. Kang et al. (2014) showed that a localized energetic forcing in the tropics shifts rainfall most strongly in the area where there is forcing and slightly westward, while localized energetic forcing in the extratropics leads to a zonally symmetric shift in precipitation. The localized response is attributed to cloud responses and easterly trade winds. Since the primary source of dust is from tropical and subtropical North Africa, and this dust creates local surface cooling, this is likely why the shift in precipitation is strongest in the Atlantic. Further simulations could quantify the impact of specific dust sources such as North Africa by adjusting the emission of individual dust sources. That the relationship remains significant everywhere, however, indicates that in addition to the local effect of Saharan dust there is also a global shift of the ITCZ from the cumulative hemispheric asymmetry.

The simulations we have shown here can be used to better understand the effects of past hemispheric dust asymmetries. As an example, there were large changes in dust emission in one or both hemispheres as the climate moved from the LGM, when dust emission was very high in both hemispheres, through the Younger Dryas and the African Humid Period, to the present. During the Younger Dryas, dust emission was greatly reduced in the Southern Hemisphere while the Northern Hemisphere remained very dusty, and during the African Humid Period dust emission in the Northern Hemisphere was greatly reduced as the wet and vegetated Sahara dramatically reduced dust emission from North Africa. While the simulations are not intended to be perfect analogues of these periods, one can view the N5S5 simulation, the N5S0 simulation, and the N0S1 simulation respectively as representing this sequence of asymmetries. Our results show that the dust forcing associated with those climatic shifts would create a southward shift in tropical precipitation relative to the preindustrial during the LGM, even more southerly precipitation during the Younger Dryas, and then a northward shift in tropical precipitation from the Younger Dryas to the mid-Holocene. This is in broad agreement with paleoproxy measurements of Atlantic ITCZ location from marine sediments in the equatorial Atlantic (Arbuszewski et al., 2013) and Cariaco basin (Haug et al., 2001). While these climate shifts were primarily the result of orbital and glacial forcings rather than dust, the agreement in sign of the precipitation shifts indicates that the dust response to the change in climate would act as a positive feedback, amplifying the change in ITCZ location.

Paleorecords of dust provide information about the relative concentration of dust deposited at a site, but without a model, this does not directly translate to a hemispheric radiative forcing or cross-equatorial heat transport. This problem can be addressed by using a subset of our experiments to inform the expected shift of the precipitation centroid due to a relative change in dust load. Using the N0S0, N1S1, N2S2, and N5S5 experiments, we can calculate the shift of the precipitation centroid per unit of the global emission multiplier. We can also calculate the effect of changing the emission multiplier in a single hemisphere, using the N0S0, N1S0, N2S0, and N5S0 or N0S0, N0S1, N0S2, and N0S5 experiments for the Northern Hemisphere or Southern Hemisphere, respectively. Scaling Northern Hemisphere dust emission produces significant results globally and in all ocean basins (Table 1). In the Atlantic and Pacific basins, we find significant shifts of $-0.35°$/unit and $-0.37°$/unit, respectively. This is to say that for each 100% change in Northern Hemisphere dust (relative to the preindustrial), a southward shift of 0.35° in the Atlantic and 0.37° in the Pacific would be expected. Ocean sediment cores from the central Pacific show dust fluxes three times greater than the preindustrial during the Last Glacial Maximum (Jacobel et al., 2017). Our results imply a 1.11° southward shift of the Pacific ITCZ and 1.05° in the Atlantic, during that time due to dust forcing, compared to observations of at least 2.5° in the Pacific (Reimi & Marcantonio, 2016) and 7° in the Atlantic (Arbuszewski et al., 2013). The magnitude of the dust-induced shifts is secondary to the large shifts due to orbital and ice sheet forcing during the LGM but still contributes roughly 15% of the Atlantic shift and possibly more than that in the Pacific. Sediment cores from the western coast of Africa found that dust fluxes during the African Humid Period were roughly five times less than during the preindustrial (McGee et al., 2013). Our results suggest a northward shift of 0.13° globally, compared to an estimated 0.3° global shift (McGee et al., 2014). Scaling the dust emission in the Southern Hemisphere alone does not produce significant shifts in our results (Table 1), likely due to the smaller contributions of southern dust to the global dust load. The strength of these relationships provides a way to estimate the precipitation shift that would be expected from an observed change in the relative concentration of dust in paleorecords, as well as in future scenarios, when even small changes to the location of the ITCZ may have large impacts on people living in the tropics.

Dust-induced shifts in tropical precipitation may generate additional climate feedbacks through processes that are not simulated in CM3. Tropical precipitation has been found to control dust deposition in the Atlantic (Van der Does et al., 2019), and once deposited in the ocean dust plays an important role in biogeochemical cycles, leading to phytoplankton blooms (Jickells et al., 2005) which alter ocean color. Changes to ocean color affect the amount of sunlight absorbed by the ocean, altering ocean temperatures, and even affecting the distribution of tropical cyclones (Gnanadesikan et al., 2010), and consequently dust wet deposition and lifetime. These processes and feedbacks could be explored using an earth system model such as ESM 4 (Dunne et al., 2020) that fully simulates dust contribution to the ocean biogeochemistry.

Climate models typically do not include decadal to millennial scale variability of dust load (Mahowald et al., 2010). Without dust variability, the climate response and balance of tropical precipitation may be biased toward the north or south depending on interhemispheric dust load. Additionally, changes of precipitation may feedback positively on dust emission, amplifying the response. Climate models that do not represent long-term dust variability thus likely underestimate the range in tropical precipitation responses. Including the effects of dust and dust variability will also be important for accurately modeling future scenarios, when dust responses to global warming will likely not be uniform between hemispheres.

Acknowledgments
We are grateful to Aaron Donohoe and Brian Rose for valuable conversations during the development of this manuscript and to Tom Delworth and Yi Ming for comments provided for an early draft. This research has been funded by the RENEW Institute at the University at Buffalo, the NOAA Ernest F. Hollings Undergraduate Scholarship, and the Carbon Mitigation Initiative of the Princeton Environmental Institute at Princeton University. Data products are archived at the University of Buffalo library (http://hdl.handle.net/10477/82087).

References

Adkins, J., deMenocal, P., & Eshel, G. (2006). The "African humid period" and the record of marine upwelling from excess ^{230}Th in Ocean Drilling Program Hole 658C. *Paleoceanography*, *21*, PA4203. https://doi.org/10.1029/2005PA001200

Allen, R. J., Sherwood, S. C., Norris, J. R., & Zender, C. S. (2012). Recent Northern Hemisphere tropical expansion primarily driven by black carbon and tropospheric ozone. *Nature*, *6*(11), 959–962. https://doi.org/10.1038/ngeo1961

Arbuszewski, J. A., deMenocal, P. B., Cléroux, C., Bradtmiller, L., & Mix, A. (2013). Meridional shifts of the Atlantic intertropical convergence zone since the last glacial maximum. *Nature Geoscience*, *6*, 959–962. https://doi.org/10.1038/ngeo1961

Balkanski, Y., Schulz, M., Claquin, T., & Guibert, S. (2007). Reevaluation of mineral aerosol radiative forcings suggests a better agreement with satellite and AERONET data. *Atmospheric Chemistry and Physics*, *7*(1), 81–95. https://doi.org/10.5194/acp-7-81-2007

Broccoli, A. J., Dahl, K. A., & Stouffer, R. J. (2006). Response of the ITCZ to Northern Hemisphere cooling. *Geophysical Research Letters*, *33*, L01702. https://doi.org/10.1029/2005GL024546

Chiang, J. C. H., Biasutti, M., & Battisti, D. S. (2003). Sensitivity of the Atlantic intertropical convergence zone to last glacial maximum boundary conditions. *Paleoceanography*, *18*(4), 1094. https://doi.org/10.1029/2003PA000916

Chiang, J. C. H., & Bitz, C. M. (2005). Influence of high latitude ice cover on the marine Intertropical Convergence Zone. *Climate Dynamics*, *25*(5), 477–496. https://doi.org/10.1007/s00382-005-0040-5

Claquin, T., Schulz, M., Balkanski, Y., & Boucher, O. (1998). Uncertainties in assessing radiative forcing by mineral dust. *Tellus Series B*, *50*(5), 491–505. https://doi.org/10.1034/j.1600-0889.1998.t01-2-00007

Claquin, T., Schulz, M., & Balkanski, Y. J. (1999). Modeling the mineralogy of atmospheric dust sources. *Journal of Geophysical Research*, *104*(D18), 22,243–22,256. https://doi.org/10.1029/1999JD900416

Di Biagio, C., Formenti, P., Balkanski, Y., Caponi, L., Cazaunau, M., Pangui, E., et al. (2017). Global scale variability of the mineral dust long-wave refractive index: A new dataset of in situ measurements for climate modeling and remote sensing. *Atmospheric Chemistry and Physics*, *17*(3), 1901–1929. https://doi.org/10.5194/acp-17-1901-2017

Donner, L. J., Wyman, B. L., Hemler, R. S., Horowitz, L. W., Ming, Y., Zhao, M., et al. (2011). The dynamical core, physical parameterizations, and basic simulation characteristics of the atmospheric component AM3 of the GFDL global coupled model CM3. *Journal of Climate*, *24*(13), 3484–3519. https://doi.org/10.1175/2011JCLI3955.1

Donohoe, A., Marshall, J., Ferreira, D., & McGee, D. (2013). The relationship between ITCZ location and cross-equatorial heat atmospheric heat transport: From the seasonal cycle to the Last Glacial Maximum. *Journal of Climate*, *26*(11), 3597–3618. https://doi.org/10.1175/JCLI-D-12-00467.1

Dunne, J., Horowitz, L. W., Adcroft, A. J., Ginoux, P., Held, I. M., John, J. G., et al. (2020). The GFDL Earth System Model version 4.1 (GFDL-ESM 4.1): Model description and simulation characteristics. *Journal of Advances in Modeling Earth Systems*, *12*, e2019MS002015. https://doi.org/10.1029/2019MS002015

Evans, S., Ginoux, P., Malyshev, S., & Shevliakova, E. (2016). Climate-vegetation interaction and amplification of Australian dust variability. *Geophysical Research Letters*, *43*, 11,823–11,830. https://doi.org/10.1002/2016GL071016

Evans, S., Malyshev, S., Ginoux, P., & Shevliakova, E. (2019). The impacts of the dust radiative effect on vegetation growth in the Sahel. *Global Biogeochemical Cycles*, *33*, 1582–1593. https://doi.org/10.1020/2018GB006128

Fischer, H., Fundel, F., Ruth, U., Twarloh, B., Wegner, A., Udisti, R., et al. (2007). Reconstruction of millennial changes in dust emission, transport and regional sea ice coverage using the deep EPICA ice cores from the Atlantic and Indian Ocean sector of Antarctica. *Earth and Planetary Science Letters*, *260*(1–2), 340–354. https://doi.org/10.1016/j.epsl.2007.06.014

Frierson, D. M. W., & Hwang, Y. T. (2012). Extratropical influence on ITCZ shifts in slab ocean simulations of global warming. *Journal of Climate*, *25*(2), 720–733. https://doi.org/10.1175/JCLI-D-11-00116.1

Fuhrer, K., Neftel, A., Anklin, M., & Maggi, V. (1993). Continuous measurements of hydrogen peroxide, formaldehyde, calcium and ammonium concentrations along the new GRIP ice core from Summit, Central Greenland. *Atmospheric Environment*, *27*(12), 1873–1880. https://doi.org/10.1016/0960-1686(93)90292-7

Fuhrer, K., Wolff, E. W., & Johnsen, S. J. (1999). Timescales for dust variability in the Greenland Ice Core Project (GRIP) ice core in the last 100,000 years. *Journal of Geophysical Research*, *104*(D24), 31,043–31,052. https://doi.org/10.1029/1999JD900929

Ginoux, P. (2017). Atmospheric chemistry: Warming or cooling dust? *Nature Geoscience*, *10*(4), 246–248. https://doi.org/10.1038/ngeo2923

Ginoux, P., Prospero, J. M., Gill, T. E., Hsu, N. C., & Zhao, M. (2012). Global-scale attribution of anthropogenic and natural dust sources and their emission rates based on MODIS Deep Blue aerosol products. *Reviews of Geophysics*, *50*, RG3005. https://doi.org/10.1029/2012RG000388

Gnanadesikan, A., Emanuel, K., Vecchi, G. A., Anderson, W. G., & Hallberg, R. (2010). How ocean color can steer Pacific tropical cyclones. *Geophysical Research Letters*, *37*, L18802. https://doi.org/10.1029/2010GL044514

Haug, G. H., Konrad, K. A., Sigman, D. M., Peterson, L. C., & Röhl, U. (2001). Southward migration of the Intertropical Convergence Zone through the Holocene. *Science*, *293*(5533), 1304–1308. https://doi.org/10.1126/science.1059725

Hoose, C., Lohmann, U., Erdin, R., & Tegen, I. (2008). The global influence of dust mineralogical composition on heterogeneous ice nucleation in mixed-phase clouds. *Environmental Research Letters*, *3*(2), 025003. https://doi.org/10.1088/1748-9326/3/2/025003

Huneeus, N., Schulz, M., Balkanski, Y., Griesfeller, J., Prospero, J., Kinne, S., et al. (2011). Global dust model intercomparison in AeroCom phase I. *Atmospheric Chemistry and Physics*, *11*(15), 7781–7816. https://doi.org/10.5194/acp-11-7781-2011

Hwang, Y.-T., Frierson, D. M. W., & Kang, S. M. (2013). Anthropogenic sulfate aerosol and the southward shift of tropical precipitation in the late 20th century. *Geophysical Research Letters*, *40*, 2845–2850. https://doi.org/10.1002/grl.50502

Jacobel, A. W., McManus, J. F., Anderson, R. F., & Winckler, G. (2016). Large deglacial shifts of the Pacific Intertropical Convergence Zone. *Nature Communications*, *7*(1), 10,499–11. https://doi.org/10.1038/ncomms10449

Jacobel, A. W., McManus, J. F., Anderson, R. F., & Winckler, G. (2017). Climate-related response of dust flux to the central equatorial Pacific over the last 150 kyr. *Earth and Planetary Science Letters*, *457*, 160–172. https://doi.org/10.1016/j.epsl.2016.09.042

Jickells, T., An, Z. S., Andersen, K. K., Baker, A. R., Bergametti, G., Brooks, N., et al. (2005). Global iron connections between dust, ocean biogeochemistry and climate. *Science*, *308*(5718), 67–71. https://doi.org/10.1126/science.1105959

Kang, S. M., Frierson, D. M. W., & Held, I. M. (2009). The tropical response to extratropical thermal forcing in an idealized GCM: The importance of radiative feedbacks and convective parameterization. *Journal of the Atmospheric Sciences*, *66*(9), 2812–2827. https://doi.org/10.1175/2009JAS2924.1

Kang, S. M., Held, I. M., Frierson, D. M., & Zhao, M. (2008). The response of the ITCZ to extratropical thermal forcing: Idealized slab-ocean experiments with a GCM. *Journal of Climate*, *21*(14), 3521–3532. https://doi.org/10.1175/2007JCLI2146.1

Kang, S. M., Held, I. M., & Xie, S. P. (2014). Contrasting the tropical responses to zonally asymmetric extratropical and tropical thermal forcing. *Climate Dynamics*, *42*(7–8), 2033–2043. https://doi.org/10.1007/s00382-013-1863-0

Kohfeld, K. E., & Harrison, S. P. (2001). DIRTMAP: The geological record of dust. *Earth-Science Reviews*, *54*, 816–114.

Kok, J. F., Ridley, D. A., Zhou, Q., Miller, R. L., Zhao, C., Heald, C. L., et al. (2017). Smaller desert dust cooling effect estimated from analysis of dust size and abundance. *Nature Geoscience*, *10*(4), 274–278. https://doi.org/10.1038/ngeo2912

Li, L., Mahowald, N. M., Miller, R. L., Garcia-Pando, C. P., Klose, M., Hamilton, D. S., et al. (2020). Quantifying the range of the dust direct radiative effect due to source mineralogy uncertainty. *Atmospheric Chemistry and Physics Discussions*.

Mahowald, N. M., Kloster, S., Engelstaedter, S., Moore, J. K., Mukhopadhyay, S., McConnell, J. R., et al. (2010). Observed 20th century desert dust variability: Impact on climate and biogeochemistry. *Atmospheric Chemistry and Physics*, *10*(22), 10,875–10,893. https://doi.org/10.5194/acp-10-10875-2010

McGee, D., deMenocal, P. B., Winckler, G., Stuut, J. B. W., & Bradtmiller, L. I. (2013). The magnitude, timing and abruptness of changes in North African dust deposition over the last 20,000 yr. *Earth and Planetary Science Letters*, *371–372*, 163–176. https://doi.org/10.1016/j.epsl.2013.03.054

McGee, D., Donohoe, A., Marshall, J., & Ferreira, D. (2014). Changes in ITCZ location and cross-equatorial heat transport at the Last Glacial Maximum, Heinrich Stadial 1, and the mid-Holocene. *Earth and Planetary Science Letters*, *390*, 69–79. https://doi.org/10.1016/j.epsl.2013.12.043

McTainsh, G. H., Tews, E. K., Leys, J. F., & Bastin, G. (2007). Spatial and temporal trends in wind erosion of Australian rangelands during 1960 to 2005 using the Dust Storm Index (DSI), Australian Collaborative Rangeland Information System. Commonwealth of Australia.

Miller, R. L., Tegen, I., & Perlwitz, J. (2004). Surface radiative forcing by soil dust aerosols and the hydrologic cycle. *Journal of Geophysical Research*, *109*, D04203. https://doi.org/10.1029/2003JD004085

Patterson, E. M., Gillette, D. A., & Stockton, B. H. (1977). Complex index of refraction between 300 and 700 nm for Saharan aerosols. *Journal of Geophysical Research*, *82*(21), 3153–3160. https://doi.org/10.1029/JC082i021p03153

Pauseta, F. S. R., Messori, G., & Zhang, Q. (2016). Impacts of dust reduction on the northward expansion of the African monsoon during the Green Sahara period. *Earth and Planetary Science Letters*, *434*, 298–307. https://doi.org/10.1016/j.epsl.2015.11.049

Prospero, J. M., Ginoux, P., Torres, O., Nicholson, S. E., & Gill, T. E. (2002). Environmental characterization of global sources of atmospheric soil dust identified with the Nimbus 7 Total Ozone Mapping Spectrometer (TOMS) absorbing aerosol product. *Reviews of Geophysics*, *40*(1), 1002. https://doi.org/10.1029/2000RG000095

Prospero, J. M., & Lamb, P. J. (2003). African droughts and dust transport to the Caribbean: Climate change implications. *Science*, *302*(5647), 1024–1027. https://doi.org/10.1126/science.1089915

Reimi, M. A., & Marcantonio, F. (2016). Constraints on the magnitude of the deglacial migration of the ITCZ in the Central Equatorial Pacific Ocean. *Earth and Planetary Science Letters*, *453*, 1–8. https://doi.org/10.1016/j.epsl.2016.07.058

Sagoo, N., & Storelvmo, T. (2017). Testing the sensitivity of past climates to the indirect effects of dust. *Geophysical Research Letters*, *44*, 5807–5817. https://doi.org/10.1002/2017GL072584

Sinyuk, A., Torres, O., & Dubovik, O. (2003). Combined use of satellite and surface observations to infer the imaginary part of refractive index of Saharan dust. *Geophysical Research Letters*, *30*(2), 1081. https://doi.org/10.1029/2002GL016189

Strong, J. D., Vecchi, G. A., & Ginoux, P. (2015). The response of the tropical Atlantic and West African climate to Saharan dust in a fully coupled GCM. *Journal of Climate*, *28*(18), 7071–7092. https://doi.org/10.1175/JCLI-D-14-00797.1

Strong, J. D., Vecchi, G. A., & Ginoux, P. (2018). The climatological effect of Saharan dust on global tropical cyclones in a fully coupled GCM. *Journal of Geophysical Research: Atmospheres*, *123*, 5538–5559. https://doi.org/10.1029/2017JD027808

Van der Does, M., Brummer, G. A., van Crimpen, F. C. J., Korte, L. F., Mahowald, N. M., Merkel, U., et al. (2019). Tropical rains controlling deposition of Saharan dust across the North Atlantic Ocean. *Geophysical Research Letters*, *47*, e2019GL086867. https://doi.org/10.1029/2019GL086867

Volz, F. E. (1973). Infrared optical constants of ammonium sulfate, Sahara dust, volcanic pumice, and flyash. *Applied Optics*, *12*(3), 564–568. https://doi.org/10.1364/AO.12.000564

Washington, R., Todd, M. C., Lizcano, G., Tegen, I., Flamant, C., Koren, I., et al. (2006). Links between topography, wind, deflation, lakes and dust: The case of the Bodele Depression, Chad. *Geophysical Research Letters*, *33*, L09401. https://doi.org/10.1029/2006GL025827